Chapter 3
Relationships Between the Skull and the Face for Forensic Craniofacial Superimposition

3.1 Introduction

The evaluation of any superimposition is a significant issue that is dependent on the consistency of the anatomical link between the location of the soft tissue surfaces relative to the underlying bone (Taylor and Brown 1998).

In order to evaluate this consistency, a full comprehension of the anatomy of the skull and the relationship between the skull and the face are required. In biological organisms, structure and function are closely related. The human head, in terms of function, is related to four of the five senses: stereoscopic vision (eyes), audition (ears), gustation (tongue/mouth), and olfaction (nose), along with the protection of the brain. These functions are responsible for the structure of the head, and therefore the form of the face and the skull will be directly related to the position of the brain, eyes, ears, mouth, and nose.

From an anthropological perspective, the reliability of CFS and an identification based on this technique are evaluated mainly on the basis of the consistency between the anatomical structures of the face and skull.

The forensic expert usually relies on the analysis of anatomical criteria such as the soft tissue thickness, outlines, and positional relationships between the skull and the face. In the scientific literature, there are several studies conducted to assess the quality/degree of matching in CFS as well as to examine the criteria used to conduct this assessment. Before reviewing the different studies, Martin and Saller's studies (1957) must be considered. They created a treatise in which the fundamental pillars of this discipline were established. They defined an important set of craniometric and somatometric points (Tables 3.1, 3.2, and 3.3) that are crucial for all anthropological studies (Figs. 3.1, 3.2, 3.3, 3.4, 3.5, and 3.6).

A correct evaluation of anatomical consistency between facial and cranial structures is of paramount importance for reliable CFS. Generating accurate data on soft tissue thickness and the positioning of facial structures are important steps to improve current practices in craniofacial identification. At the moment, there is a

S. Damas et al., *Handbook on Craniofacial Superimposition*,
https://doi.org/10.1007/978-3-319-11137-7_3

Table 3.1 Craniometric points from Martin (1914) study (neurocranium)

Craniometric points: neurocranium					
ast	asterion	ft	frontotemporale	ms	mastoideale
au	auriculare	g	glabella	o	opisthion
b	bregma	i	inion	op	opisthocranion
ba	basion	l	lambda	po	porion
eu	euryon	m	metopion	so	supraorbitale

Taken from Martin and Saller (1957)

Table 3.2 Craniometric points from Martin (1914) study (splanchnocranium)

Craniometric points: splanchnocranium					
d	dacryon	n	nasion	rhi	rhinion
gn	gnathion	ns	nasospinale	zo	zygoorbitale
go	gonion	or	orbitale	zm	zygomaxillare
ml	mentale	pg	pogonion	zy	zygion
mf	maxillo-frontale	pr	prosthion		

Taken from Knußmann (1988)

Table 3.3 Somatometric points from Martin (1914) study

al	alare	g	glabellare	ma	mastoidale	pr	prosthion
cdl	condylion laterale	go	gonion	n	nasion	prn	pronasale
ch	cheilion	I	inion	or	orbitale	ps	palpebrale superius
en	endocanthion	labm	labiomentale	os	orbitale superius	sa	superaulare
eu	euryon	li	labrale inferius	pg	pogonion	sba	subaurale
ex	exocanthion	ls	labrale superius	pi	palpebral inferius	sci	superciliare
ft	frontotemporale	m	metopion	po	porion	se	sellion
gn	gnathion	op	opisthocranion	pu	pupilare	sn	subnasale
sto	stomion	t	tragion	tr	trichion	v	vertex
zy	zygion						

Taken from Knußmann (1988)

clear lack of consensus in methodological approaches for CFS. The development of standard protocols is necessary to enhance the credibility of the technique, making it more readily admissible in judicial processes.

3.2 Anthropometrical Relationships

Understanding the relationship between the skull and the facial soft tissue has major relevance for forensic identification. Facial soft tissue thickness, measured as the distance from the skin surface to the most superficial surface of the underlying

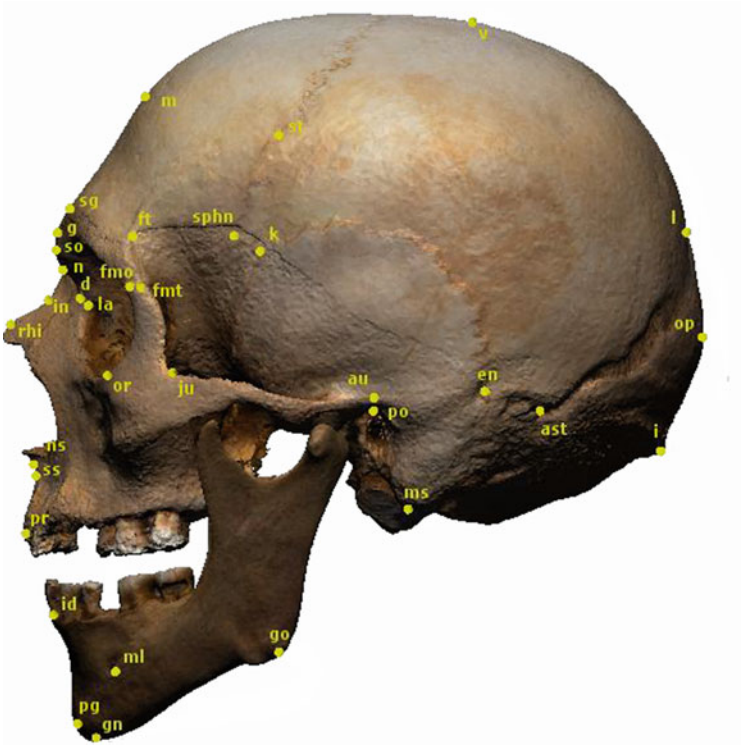

Fig. 3.1 Craniometric points in lateral view. Taken from Knußmann (1988)

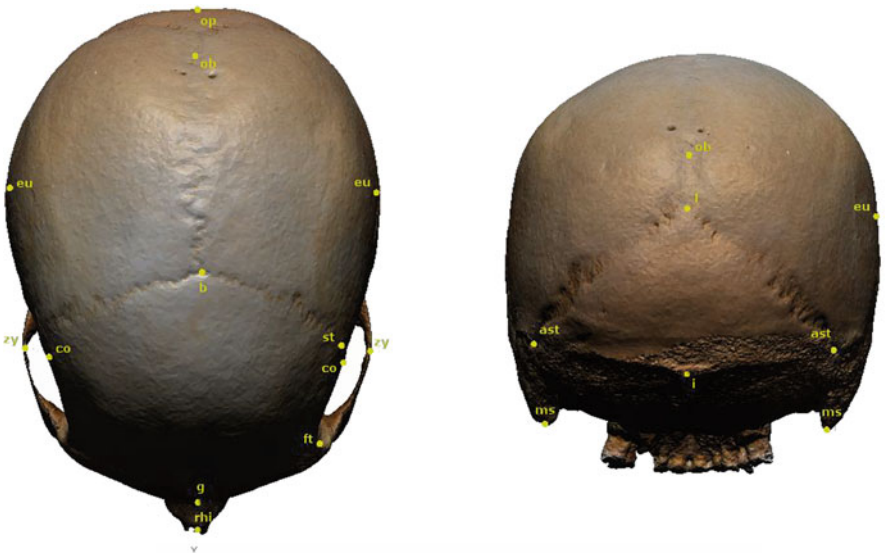

Fig. 3.2 Craniometric point in vertical view (left) and in occipital view (right). Taken from Knußmann (1988)

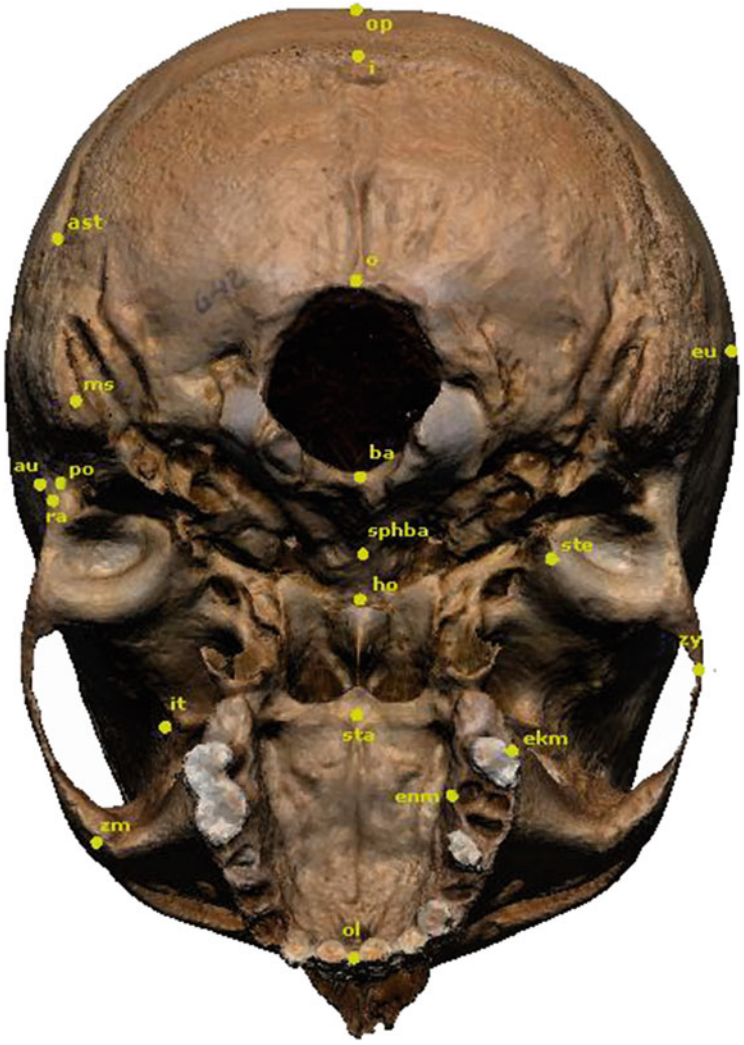

Fig. 3.3 Craniometric points in basilar view. Taken from Knußmann (1988)

skeletal tissue at specific landmarks, provides an important criterion for the evaluation of anatomical consistency. This kind of measurement provides general information on the match between the face and the skull, using facial soft tissue thickness as a means to control the outer contour of the face during the superimposition (Codinha and Fialho 2010; Stephan and Simpson 2008).

Due to the scientific value of facial soft tissue thickness in craniofacial identification, numerous studies have been conducted since 1883, with a great variation in measuring techniques, sample size, population ancestry, anatomical landmarks, and variables analyzed (e.g., sex, age, and body composition) (Codinha and Fialho 2010; Stephan and Simpson 2008).

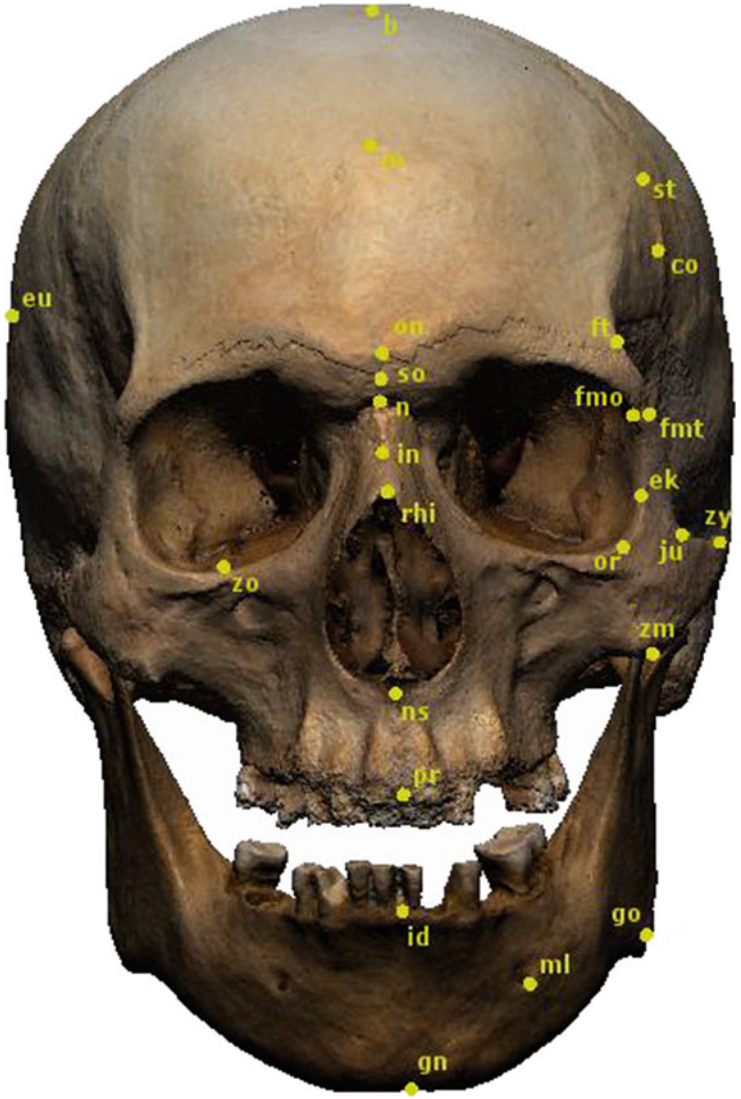

Fig. 3.4 Craniometric points in frontal view. Taken from Knußmann (1988)

Some of the main modalities for soft tissue thickness acquisition mentioned in the literature include:

- Needle puncture (Codinha and Fialho 2010; Simpson and Henneberg 2002; Domaracki and Stephan 2006; Rhine and Campbell 1980; Suzuki 1948; Birkner 1905; Stadtmuller 1925; Rhine et al. 1982; Galdames et al. 2008; His 1895; von Eggeling 1909)

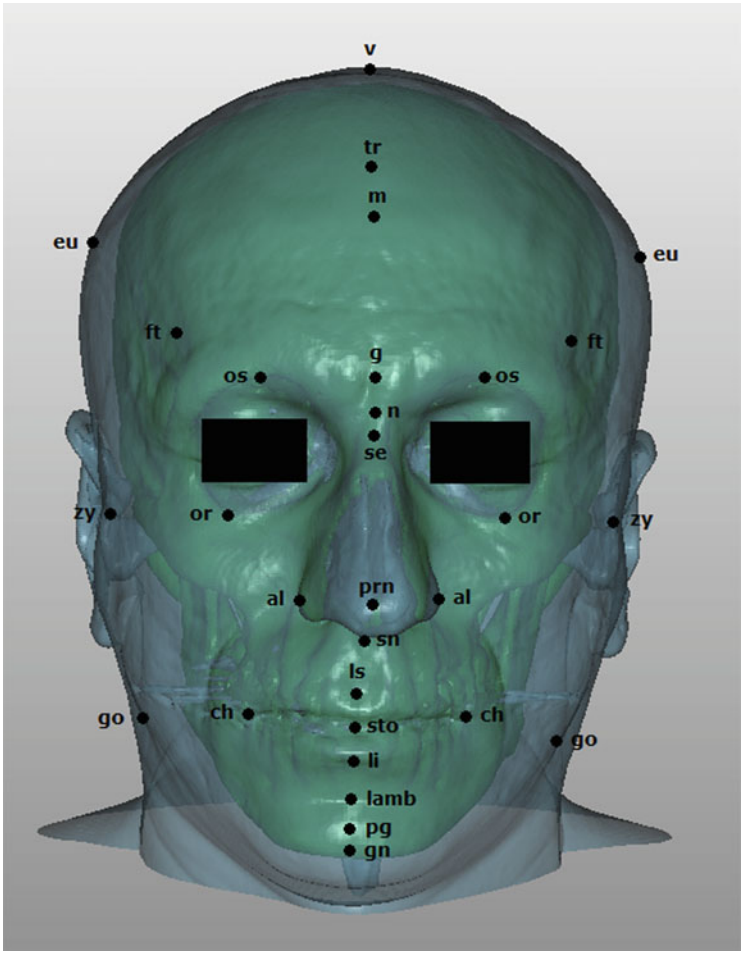

Fig. 3.5 Somatometric points in frontal view

- Cephaloradiography (George 1987; Leopold 1968; Weinig 1958; Bankowski 1958)
- Ultrasound imaging (Aulsebrook et al. 1996; Wilkinson 2002)
- Computer-assisted tomography (CT) (Phillips and Smuts 1996)
- Cone-beam CT (Bankowski 1958)
- Magnetic resonance imaging (Sahni 2002)

A summary of the most important soft tissue thickness studies and their main characteristics are listed in Table 3.4. None of these methodologies offer a perfect solution, as each technique has advantages and disadvantages. For example, needle puncture methods are inexpensive, but cadaveric material is not wholly

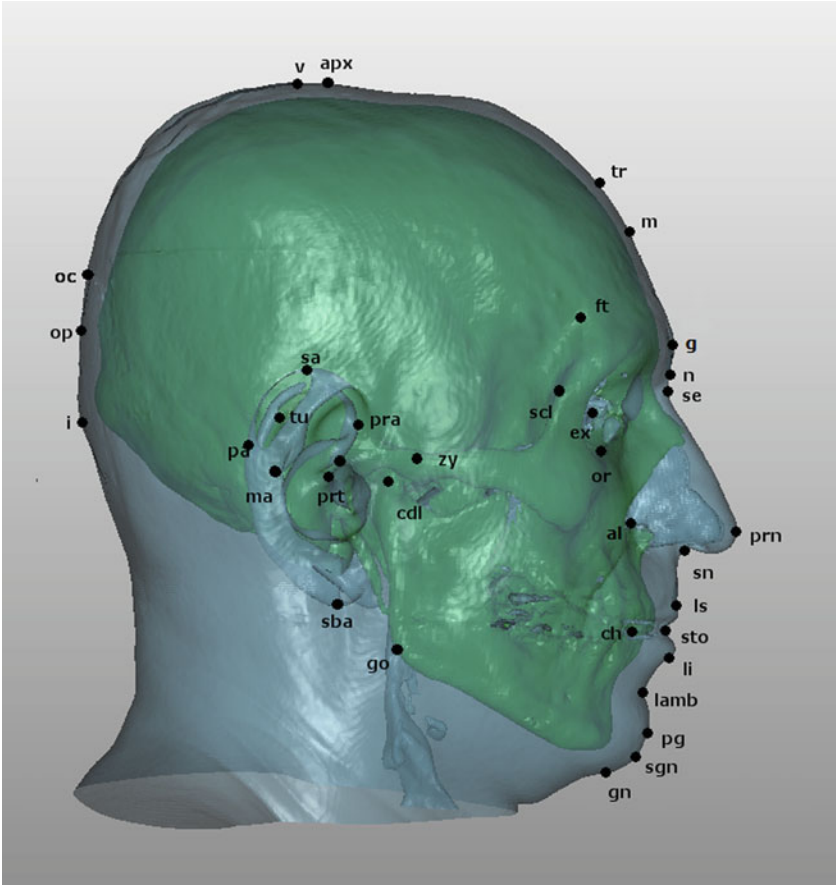

Fig. 3.6 Somatometric points in lateral view

representative of living subjects; CT scans are accurate and reproducible but may present gravity effects on the supine face, artifacts, and radiation damage; craniographs are inexpensive and the subject is upright, but the images can suffer from magnification and planar issues; ultrasound can be used on upright living subjects but involves contact and pressure issues. A more extensive list of advantages and disadvantages of the different methodologies used in soft tissue data collection was analyzed in Stephan and Simpson (2008) and in Preedy (2012). The latter is summarized in Tables 3.5 and 3.6.

The soft tissue thickness depth measurements are applied in facial depiction, but if they are used in CFS, changes due to facial expression must also be considered when determining identity. These measurements are usually, but not always, perpendicular to the bony structures, and are most useful if the image shows the soft tissue directly to the point of measurement (Clement and Ranson 1998).

Table 3.4 Landmarks used by authors, sample, and methodology

Reference	Date	Number of points	Male	Female	Total	Population[a]	Methods
Welcker	1883	7	13		13	White (Cadavers)	Tissue puncture by using needle
His	1895	15	24	4	28	White (Cadavers)	Tissue puncture by using needle
Kollmann and Buchly	1898	18	21	4	25	White European (Cadavers)	Tissue puncture by using needle
Fischer	1905	18	2		2	Mongoloid (Papuans)	Tissue puncture by using needle
Birkner	1905	18	9		6	Mongoloid (Chinese)	Tissue puncture by using needle
Czekanowski	1907	6	64	51	112	White Caucasian (Cadavers)	Tissue puncture by using needle
Von Eggeling	1909	18	3		3	Black (Hererons)	Tissue puncture by using needle
Stadtmuller	1923–1925	20	15	3	18	Mongoloid, White	Tissue puncture by using needle
Suzuki	1948	18	7	48	55	Mongoloid (Japanese)	Tissue puncture by using needle
Weinig	1958	10	99	21	120	White Americans (Living)	Craniographs
Bankowski	1958	13	15	9	24	White Europeans (Living)	Craniographs
Berger	1965	14	26	102	128	White Caucasian (Cadavers)	Tissue puncture by using needle
Leopold	1968	13	102	52	154	White Europeans (Cadavers)	Craniographs
Sutton	1969				104	White Caucasian (Cadavers)	Tissue puncture by using needle
Rhine and Campbell	1980	21	44	15	59	American Black (Unembalmed cadavers)	Needle and rubber-stopper technique

(continued)

Table 3.4 (continued)

Reference	Date	Number of points	Male	Female	Total	Population[a]	Methods
Farkas	1981	132				White (Caucasian North American population)	
Rhine et al.	1982	21	37	19	56	American White Caucasian (Unembalmed cadavers)	Tissue puncture by using needle
Rhine	1983	21	9	2	11	South-western Indians (Cadavers)	Tissue puncture by using needle
Helmer	1984	34	61	62	123	White European (Living)	Ultrasound
Hodson et al.	1985	20			50	American Caucasians	Ultrasound
Dumont	1986	9	93	101	194	Caucasian	X-Ray
George	1987	10	17	37	54	Whites American (Living)	Lateral craniographs
Nanda and Meng	1990	4	17	23	40	Caucasian	X-Ray
Aulsebrook et al.	1996	–	55		55	Zulu (Living) Negroids	Lateral, oblique cephalometry ultrasound
Phillips and Smuts	1996	21	16	16	32	Mixed raced South Africans (Living)	Computerized tomography
Manhein and Listi	2000	19			712	American	Ultrasound
El-Mehallawi and Soliman	2001	17	120	84	204	Egyptian (Living)	Ultrasound
El-Mehallawi and Soliman	2001	17	120	84	204	Egyptian	Ultrasound
Sahni	2002	19	30	30	60	Indians (Living)	MRI scans
Simpson and Henneberg	2002	20	17	23	40	Australian	Tissue puncture by using needle
Wilkinson	2002	21	99	101	200	British Juveniles	Ultrasonic echo-location
Williamson and Nawrocki	2002	15	77	147	224	African American	X-Ray
Utsuno and Kageyama	2005	12	0	112	112	Japanese	X-Ray

(continued)

Table 3.4 (continued)

Reference	Date	Number of points	Male	Female	Total	Population[a]	Methods
De Greef et al.	2006	52	510	457	967	White Caucasian (Living)	Ultrasound
Domaracki and Stephan	2006	13	19	14	33	Australian	Tissue puncture by using needle
Vander Pluym et al.	2007	–	5	5	10	American (multiple ancestries)	MRI
Panenková	2007	14	80	80	160	Slovak	CT Scan
Galdames et al.	2008	14	30		30	Cadavers	Tissue puncture by using needle
Sahni et al.	2008	29	173	127	300	Indian	MRI
Inada et al.	2009		40	40	80	Mongoloid (Japanese) (Living)	Cephalograms
Codinha and Fialho	2010	20	103	48	151	Portuguese	Tissue puncture by using needle
Menezes et al.	2009	50	531	357	888		Electronic digitizer
Tedeschi-Oliveira et al.	2009	11	26	14	40	Brazilian	Tissue puncture by using needle
Cavanagh and Steyn	2011	28	0	154	154	South African	CT Scan
Saxena et al.	2012	7	19	21	40	Indian	CT Scan
Hwang et al.	2012	31	50	50	100	Korean	CT Scan

[a]Population as described by the authors

Other factors that must be taken into account when utilizing soft tissue data are growth, weight change, and age-related changes. For this purpose, many authors place emphasis on facial features with minimal soft tissue depth. The middle third of the face (eyes, nose, and teeth) is less influenced by any photographic distortion and could be considered more accurate (Taylor and Brown 1998).

Currently, there is no agreement among practitioners as to the number of landmarks, their name, or their correct position; thus, comparison between the results of several papers is extremely difficult (Panenková 2007). Furthermore, some papers use the vernacular rather than anatomical terminology, that is, "end of nasal" (Phillips and Smuts 1996), "middle of the bony nose" (Helmer 1984), and "angle of mouth" (Aulsebrook et al. 1996; Panenková 2007).

There seems to be one major difference of opinion with regard to the thicknesses of facial tissues (Wilkinson 2002). The results obtained by the needle puncture method in cadavers are relative to the process of dehydration of the soft tissue (10–18 g/day/weight), resulting in considerable variations depending on the

Table 3.5 Comparison of the commonly used measuring techniques for calculating soft-tissue depth

Method of measurement	Advantage	Disadvantage
Needle puncture	Low cost. Operating characteristics well defined. Measurements can be made in Frankfort. Horizontal plane.	Invasive. Most information from cadavers, soft tissue may not accurately reflect living tissue. Compression of soft tissue inevitable during measurement. No visualization of the skeletal surface.
Plain film radiography	Standard cephalograms widely used in dentistry and medicine. Films generally taken in Frankfort horizontal plane. Relatively inexpensive. No compression of tissue while taking measurement.	Exposure to ionizing radiation, patient selection may bias results. Only useful where surface landmark and bony landmark are parallel to the film plate. Metallic implants (braces and fillings) may interfere with measurements. Magnification issues.
Computerized tomography	Widely used in medicine and dentistry. Images are digital and easy to manipulate (e.g., absorption characteristic of soft and hard tissue relatively easy to distinguish). Accuracy of surface landmark placement relative to bony landmark can be verified. Paired landmarks easily measured. Known accuracy and reproducibility.	Expensive. Requires exposure to ionizing radiation, patient selection may introduce bias. Patient motion artifact (voluntary or involuntary) may interfere with measurements. Radio-opaque objects (e.g., filling, braces) may distort images and measurements. Images are not in Frankfort horizontal plane. Gravity effects on soft tissue due to supine position. Translation to 3D shape may involve manual intervention.
Magnetic Resonance Imaging	No exposure to ionizing radiation, ethically acceptable to image subjects for tissue depth estimation. Can be repeated on same subjects to obtain longitudinal data. No soft-tissue compression during measurement Images are digital and easy to manipulate (e.g. absorption characteristics of soft and hard tissue relatively easy to distinguish). Accuracy of surface landmark placement relative to bony landmark can be verified. Paired landmarks easily measured.	Very expensive. Images generally not acquired in Frankfort horizontal plane. Requires exposure to high-intensity magnetic field, subjects with metallic exposure not eligible. Subject motion artifact distorts images. May not visualize bone well. Gravity effects due to supine position. Translation to 3D shape may involve manual intervention.

(continued)

Table 3.5 (continued)

Method of measurement	Advantage	Disadvantage
Ultrasound	No exposure to ionizing radiation; can be used repeatedly in the same subject. Portable, can be used in the field. Measurements made in Frankfort horizontal plane.	Probe must touch skin surface, tissue compression possible with inexperienced operator. Operating characteristics of portable equipment differ according to manufacturer and must be defined before use. Difficult to scan parallel to skeletal surface and this can make visualization of the surface more challenging.

Taken from Taylor and Brown (1998)

Table 3.6 Systematic bias of soft-tissue measurement according to method of measurements

Measurement technique	Landmarks at which tissue depths are consistently higher than with other techniques	Landmarks at which tissue depths are consistently lower than with other techniques	Measurements technique that most closely correlates
Needle puncture	–	–	–
Plain radiology	All midline landmarks	Lateral landmarks: gonion and zygion	–
CT scan	All midline landmarks	All midline points	MRI
MRI scan	–	All midline points	CT
Ultrasound	Supra M2, infra M2, gonion, mid-infraorbital, anterior masseter border	–	Needle puncture (except for supra M2)

Taken from Preedy (2012)

different methods used for conservation, alongside the development of rigor mortis, which affects the muscle fibers (Galdames et al. 2008; de Greef et al. 2006).

Various investigators have compared the soft facial tissue thicknesses measured in fresh cadavers with embalmed cadavers. Simpson and Henneberg (2002) reported an increase in soft tissue thickness of all landmarks, due to embalming processes. Galdames et al. (2008) indicated that the embalmed cadavers presented larger thicknesses of tissue in all sites, with the exception of the right exocanthion and right and left gonion points. The most significant differences between fresh and embalmed tissue were observed at the trichion, glabella, nasion, pogonion, superciliary, supraorbital, infraorbital, and gonion points (Galdames et al. 2008; Simpson and Henneberg 2002).

Postmortem data and the use of the different methods of cadaver conservation must be considered when comparing measurements with those obtained from living subjects by means of radiograph, ultrasound, computerized tomography, or nuclear magnetic resonance (Clement and Ranson 1998; Galdames et al. 2008).

3.3 Anatomical Relationships

The face is one of the most individualistic and unique parts of the human body. It is important to establish the most commonly utilized morphological features when carrying out an assessment of face and skull correspondence. There are many standards for the prediction of the soft tissue features from skeletal assessment, and these standards were established through human dissection, palpation, medical imaging modalities, and direct anthropometry of living subjects. The relative limitations of each method when evaluating the reliability of the standards produced should be noted. Human dissection studies offer a unique opportunity to visualize the face and the related skeletal structures, but are limited by the effects of embalming, deformation associated with a cadaver face, and dehydration. Palpation studies employ living faces but are limited by the inability to accurately locate bony landmarks, especially in the areas of the face with the greatest soft tissues. Clinical imaging of living faces enables the visualization of soft and hard tissues simultaneously, but different imaging modalities suffer from gravitational problems (the subject is supine), artifacts (dental flare), bone visibility (MRI), and pressure effects (ultrasound). Direct anthropometry from a living subject is probably the most reliable form of data collection, but although multiple measurements can be collected from the soft tissues, direct measurements of the skull are limited to the teeth.

This report will attempt to highlight the published anatomical standards feature by feature.

3.3.1 General Face Shape

The relationship between the shape of the head and the shape of the cranium is well established. Several classifications of this relationship have been published (Clement and Ranson 1998; Fedosyutkin and Nainys 1993; Balueva et al. 2009), Table 3.7 summarizes the standards.

The relationship between facial measurements and related skull measurements has also been studied (Balueva et al. 2009). Table 3.8 summarizes the standards.

3.3.2 The Eyebrows

Eyebrow pattern standards (Table 3.9) have been developed from a combination of palpation (Balueva et al. 2009) and craniograph studies (Fedosyutkin and Nainys 1993).

Table 3.7 Shape relationships of head and cranium

Morphological and facial traits	Correspondence with facial structures
The general head shape	
Shape of face	Transverse arc of the cranium
Rounded	Semisphere
Square	Pentagonoid
Oval	Oval
Triangular	Rectangular
	The shape of the *temporal lines* provides information about the *forehead width*
Shape of the face	Mandible
Oval	If the gonial angle is over 125° and the coronoid process is high, the lowest part of the head is likely to be narrow
Triangular	If the gonial angle is over 125° and the coronoid process is high, the lowest part of the head is likely to be narrow
Rounded	If the gonial angle is less than 125°, then the face shape is likely to be wide
Rectangular	If the gonial angle is less than 125°, then the face shape is likely to be wide
General face shape	
Rounded	Parietal part gently curved in frontal view; occiput rounded in lateral view
Dome shaped	Parietal part protruding; occiput flattened in lateral view
Egg shaped	Parietal part gently curved in frontal view; occiput protruding
Keel shaped	Parietal part narrow, laterally compressed and "sharpened" in frontal view; gently curved or protruding in lateral view; occiput rounded, flattened, or protruding
Flattened	Parietal part flattened in frontal view, flattened in lateral view; occiput rounded or protruding in lateral view
Saddle shape	Parietal part gently curved or flattened, saddle shaped in lateral view; occiput rounded, flattened, or protruding in lateral view
Face in frontal view	
Rounded	As in cranial contour; malar bones prominent; general contour rounded
Oval	As in cranial contour; facial outline smooth; general contour elliptical
Triangular	As in cranial contour; frontal part wide, mandible narrow; general contour triangular
Square	As in cranial contour; transverse dimensions large; general contour square
Rectangular	As in cranial contour; frontal and mandibular widths roughly equal; face high, outline angular; general contour rectangular
Diamond-shaped	As in cranial contour; frontal and mandibular breadth small, face broad and high; general contour diamond shaped
Vertical facial profile	
Sharp	Nasal saddle high; malar bones not prominent
Flattened	Nasal saddle low; malar bones prominent

(continued)

Table 3.7 (continued)

Morphological and facial traits	Correspondence with facial structures
Frontal curvature in profile	
Flat	Frontal outline nearly straight
Convex	Frontal outline convex arc
Concave	Both glabella and frontal tubers developed, creating the impression of concavity in the middle part
Wavy	Glabella developed, well-expressed flexure between it and the upper part of the frontal bone
Frontal angle in profile	
Vertical	Perpendicular to Frankfort horizontal plane tangent to glabella nearly vertical
Inclined backward	Perpendicular to Frankfort horizontal plane tangent to glabella inclined backward
Inclined forward	Perpendicular to Frankfort horizontal plane tangent to glabella inclined forward
Brow ridges	
Medium	Brow ridges markedly prominent, but without a depression between them
Large	Brow ridges markedly prominent and separated by depression
Small	Brow ridges barely distinguishable
Brow ridges	
Medium	Moderately prominent from side view
Large	Markedly prominent from side view
Small	Barely distinguishable from side view
Length of brow ridges	
Large	Extend beyond midpoint of supraorbital margin
Small	Do not reach midpoint of supraorbital margin

Table 3.8 Related face and skull measurements

Relative facial breadth	
Medium	(Bizygomatic (45) + 10 mm)/(supraorbitale to gnathion (47b) + 6 mm) = 1.10 ± 0.04
Large	(Bizygomatic (45) +10 mm)/(supraorbitale to gnathion (47b) + 6 mm) > 1.14
Small	(Bizygomatic (45) + 10 mm)/(supraorbitale to gnathion (47b) + 6 mm) < 1.06
Frontal height	
Medium	(Trichion to supraorbitale)/(supraorbitale to gnathion (47b) + 6 mm) = 0.45 ± 0.03
Large	(Trichion to supraorbitale)/(supraorbitale to gnathion (47b) + 6 mm) > 0.48
Small	(Trichion to supraorbitale)/(supraorbitale to gnathion (47b) + 6 mm) < 0.42
Frontal breadth	
Medium	(Bicoronal (10) + 10 mm)/(bizygomatic (45) + 10 mm) = 0.90 ± 0.02
Large	(Bicoronal (10) + 10 mm)/(bizygomatic (45) + 10 mm) > 0.92
Small	(Bicoronal (10) + 10 mm)/(bizygomatic (45) + 10 mm) < 0.88

Table 3.9 Eyebrow pattern standards

Eyebrow pattern	
Overhanging	There is a strong development of the supraorbital margin and brow ridge, the eyebrows are shifted downward, 1–2 mm lower than the supraorbital rim
Arched	This is related to a smooth forehead and high orbit, with the eyebrow following the curve of the supraorbital margin
Triangular	There is thickening of the outer part of the supraorbital rim and a strong brow ridge, the eyebrow is arranged over the supraorbital margin forming an angle
Outline of eyebrows	
Straight	Supraorbital margin straight; superciliary arch horizontal
Arched	Supraorbital margin arcuate; lateral end of superciliary arch directed upward
Broken	Supraorbital margin wavy; lateral end of superciliary arch directed upward

Table 3.10 Relationship between the eyeball and the orbit

Eyes	
Protrusion of the eyeballs	
	This is related to the depth of the orbital cavity, vertical inclination of the orbit, and the thickness and degree of overhang of its upper rim
Deep-set eye	The supraorbital rim is greatly thickened and protrudes relative to the infraorbital rim Supraorbital margin projects inferiorly ("closed orbit") (orbital height (52))/(exocanthion to endocanthion) < 0.81
Prominent eye	Supraorbital margin does not project inferiorly (orbital height (52))/(exocanthion to endocanthion) > 0.81
Eyeball prominence	Normal prominence is when the iris touches a tangent across the mid-supraorbital to mid-infraorbital bone eyeball protrusion $= 18.3 - (0.4 \times$ orbit depth)

3.3.3 The Eyes

A number of studies assessing the relationship between the eyeball and the orbit in relation to prominence and frontal position have been conducted.

Prominence studies utilizing MRI (Wilkinson and Mautner 2003) exophthalmometry (Stephan 2002), and palpation (Fedosyutkin and Nainys 1993; Balueva et al. 2009) all present results indicating a general agreement between current published standards (see Table 3.10).

Studies on the position of the eyeball in the orbit from a frontal view seem to report different results depending on the method of assessment. Dissection studies (Whitnall 1921; Stephan and Davidson 2008; Stephan et al. 2003) suggest that the eyeball sits slightly superior (1–2 mm) and lateral to the centre in the orbit, but palpation studies (Balueva and Veselovskaya 2004) suggest that the eyeball sits 2 mm closer to the medial wall than the lateral wall; other dissection studies (Krogman and İşcan 1986) suggest the eyeball sits centrally in the orbit.

The positions of the inner (endocanthus) and outer (exocanthus) corners of the eye have been studied in detail, but there is no clear agreement between standards. There is a general agreement concerning the malar (or Whitnall's) tubercle in relation to the outer canthus. Human dissection has shown that the tendons that fix the eyelids to the orbit are inserted at this tubercle (Whitnall 1921). Although it has been established that the outer canthus is located at the same height as the malar tubercle, there is no consensus as to the distance of the outer canthus from the orbital wall. The distance has been published as 1 mm (Sills 2004), 3–5 mm (Balueva et al. 2009; Angel 1978; Krogman and İşcan 1986; Stephan 2009), 5–7 mm (Wolff 1976; Rosenstein et al. 2000), 8–10 mm (Couly et al. 1976), and 13 mm (Anastassov and van Damme 1996). Where the malar tubercle is absent, the outer canthus can be positioned 8–11 mm below the line of the frontozygomatic suture (Stewart 1983; Krogman and İşcan 1986; Wolff 1976).

There is an agreement that the medial canthus is positioned approximately 2–5 mm lateral to the anterior lacrimal crest (Yoshino and Seta 1989; Angel 1978; Sills 2004; Krogman and İşcan 1986; Stephan 2009), but where exactly on the anterior lacrimal crest this measurement is taken from is unclear. Different studies suggest the top (Balueva and Veselovskaya 2004), middle (Angel 1978), and base (Fedosyutkin and Nainys 1993) as the measurement point, while other studies suggest that the point can be found 4–5 mm (Angel 1978) or 10 mm (Stewart 1983) below the dacryon. Table 3.11 presents the standards related to dissection and anthropometrical studies (Whitnall 1921; Merkel 1886).

Table 3.11 Position of the inner (endocanthus) and outer (exocanthus) corners of the eye

Eyes	
	The slope of the fissure is defined by a straight line that connects the malar (Whitnall's) tubercle on the lateral border of the orbit with the anterior lacrimal crest on the medial border of the orbit
	The curves of the eyelid margins are not symmetrical and the upper lid is more pronounced than the lower, its height being greatest nearer the medial angle, whereas that of the lower lid is nearer the lateral angle The lateral canthal angle is more acute than the medial and lies in close contact with the globe, whereas the medial canthus extends toward the nose 5–7 mm away from the globe, being separated by the caruncula and the plica semilunaris The radius of the upper eyelid curve is 16.5 mm and that of the lower eyelid is 22 mm The outer canthus (exocanthus) is positioned at the same height as the malar (Whitnall's tubercle) and medial to it Where the malar tubercle is absent, the outer canthus can be positioned 8–11 mm below the line of the frontozygomatic suture The inner canthus (endocanthus) is situated 2–5 mm lateral to the anterior lacrimal crest
Eye fissure	
	The length of the eye fissure is 60–80% of the width of the orbit
Medium	(Exocanthion to endocanthion − 14 mm)/(upper facial breadth (43) + 10 mm)= 0.25 ± 0.01
Large	(Exocanthion to endocanthion − 14 mm)/(upper facial breadth (43)+ 10 mm)> 0.26
Small	(Exocanthion to endocanthion − 14 mm)/(upper facial breadth (43)+ 10 mm)< 0.24

Table 3.12 Eyelid pattern

Eyelid patterns	
Lateral	There is an overhang in the lateral part of the supraorbital rim
Central	There is an overhang in the central part of the supraorbital rim
Upper eyelid fold	
Moderate	Supraorbital margins straight or slightly rounded
Defined	Supraorbital margins arched and sharp
Absent	Supraorbital margins arched, supraorbital overhang markedly shifted medially
Irregular	Supraorbital margin wave shaped or oblique in distal part
Epicanthic fold	
Present	Crest descending from medial supraorbital margin directed toward anterior lacrimal crest This is characteristic of a high orbit, a low-or medium-height nasal bridge, and a long lacrimal fossa
Absent	Crest descending from medial supraorbital margin directed inside orbit

The eyelid pattern has been studied using palpation and anthropometry studies (comparison of skulls with ante-mortem images) (Balueva et al. 2009; Rynn et al. 2012). These standards are presented in Table 3.12.

3.3.4 The Nose

The nose is the most studied feature on the face; studies on the relationship between the configuration of the nasal tissue and the bones surrounding the nasal aperture are abundant (Gerasimov 1955; Macho 1986; McClintock Robinson et al. 1986; George 1993; Schultz 2005; Tandler 1909; Virchow 1912; Glanville 1969; Prokopec and Ubelaker 2002; Stephan et al. 2003). Studies conducted by Gerasimov (1955) show that the soft nose is wider than the bony aperture, as a narrower soft nose would have no supporting structure. Furthermore, he suggested that the bony nasal aperture at its widest point is three-fifths of the overall width of the soft nose. This assertion has been confirmed by a CT study on living subjects of various ethnic groups (Rynn 2006).

Gerasimov (1955) also suggested that the nasal base angle (the angle between the upper lip and the columella) is determined by the direction of the nasal spine. In his study, he stated that the axis of the nasal spine serves as a base for the soft nose and the determination of the nasal spine direction follows the point of the spine, as if it were an arrowhead. He also suggested that the end of the soft nose could be predicted as the point where a line following the projection of the last part of the nasal bones (at the rhinion) crosses a line following the direction of the nasal spine, and he confirmed these standards with a blind study of 50 cadaver heads. This standard has been widely debated in the literature; Ullrich, a former student of Gerasimov, claimed that Gerasimov did not follow the direction of the nasal spine, but rather the general direction of the floor of the anterior part of the nasal aperture (maxillary

bone) laterally adjacent to the anterior nasal spine and vomer bone (Ullrich and Stephan 2011). However, this is disputed by the academic group who worked for many years alongside Gerasimov and Lebedinskaya, and continue their work at the Russian Academy of Sciences in Moscow (Balueva et al. 2009; Rynn et al. 2012) and they confirm that the nasal spine was indeed the feature used by Gerasimov to determine the nasal base angle. Rynn and Wilkinson (2006) tested six different methods of nose prominence prediction (Gerasimov 1955; Prokopec and Ubelaker 2002; Macho 1986; Stephan et al. 2003; George 1987; Krogman and İşcan 1986) in order to understand which method was the most accurate. This study found that the Gerasimov (1955) method performed with the most accuracy, while the Krogman and İşcan (1986) method performed poorly.

Rynn (2006) produced guidelines for nasal shape prediction, utilizing three cranial measurements that can be used to predict six soft nose measurements. These guidelines were tested in a blind study showing a high level of accuracy (Rynn et al. 2010).

Gerasimov (1955) also suggested that the height of the upper border of the alae is in line with the crista conchalis and the profile of the nose is a nonscaled mirror of the nasal aperture in profile. These standards have been confirmed using CT data of living subjects (Rynn 2006); this study additionally confirmed previous papers' suggestions that deviation of the nasal tip from the midline is associated with opposing nasal septum deviation (Selzter 1944; Gray 1965) and that nasal tip bifurcation is associated with a bifid nasal spine (Weaver and Bellinger 1946).

A recent dissection study suggested that the shape of the nasal aperture when viewed from posterior–anterior aspect is mirrored in the shape of the nasal tip (Davy-Jow et al. 2012). Standards for nose shape prediction are given in Table 3.13.

3.3.5 The Mouth

There are some anatomical standards relating to mouth shape, which have been confirmed in different populations and by a variety of methods of study (Stephan et al. 2003; Balueva et al. 2009; Stephan and Murphy 2008; Angel 1978; Krogman and İşcan 1986). These are presented in Table 3.14.

Scientific literature from orthodontic and anatomical disciplines suggests that the form of the mouth is related to the occlusion of the teeth (Roos 1977; Rudee 1964; Koch et al. 1979; Waldman 1982; Holdaway 1983; Denis and Speidel 1987; Talass et al. 1987), the dental pattern (Subtelny 1959), and the facial profile (Gerasimov 1955). These are presented in Table 3.14.

3.3.6 The Cheeks

Studies demonstrating the relationship between the zygomatic bones, the canine fossa, and the soft cheeks are presented in Table 3.15 (Fedosyutkin and Nainys 1993; Balueva et al. 2009).

Table 3.13 Standards for nose shape prediction

Nose	
Height of the nose	
	This equals the distance from nasion to 1–2 mm below the nasal spine
Medium	(Supraorbitale to subspinale)/(trichion to gnathion + 6 mm) = 0.32 ± 0.015
Large	(Supraorbitale to subspinale)/(trichion to gnathion + 6 mm) > 0.335
Small	(Supraorbitale to subspinale)/(trichion to gnathion + 6 mm) < 0.305
Nasal length	Europeans: nasion to prosthion = 0.74 (bony nasion to subspinale) + 3.5
Nasal length	Nasion to pronasale (mm) in nasion–prosthion plane = 0.9 (bony nasion to acanthion) – 2
Nasal height	European females: nasion to subspinale = 0.63 (bony nasion to subspinale) + 17 European males: nasion to subspinale = 0.78 (bony nasion to subspinale) + 9.5
Width of the nose	
	This is defined between the midpoints of the canines or their alveoli The maximum width of the nasal aperture is three-fifths (^{3}/5) of the maximum width of the soft nose
Medium	Nasal breadth/(bizygomatic breadth (45) + 10 mm) = 0.25 ± 0.01
Large	Nasal breadth/(bizygomatic breadth (45) + 10 mm) > 0.26
Small	Nasal breadth/(bizygomatic breadth (45) + 10 mm) < 0.24
The base of the nose	
Horizontal	Horizontal nasal spine
Elevated	Up-turned nasal spine
Prolapsed	Down-turned nasal spine
The tip of the nose	
Bifid	Bifurcated nasal spine
Nasal depth	Female; subspinale to pronasale = 0.5 (bony rhinion to subspinale) + 1.5 male; subspinale to pronasale = 0.4 (bony rhinion to subspinale) + 5
Pronasale	Anterior projection (mm) perpendicular to nasion–prosthion plane= 0.83Y − 3.5
Pronasale	Projection from subspinale in Frankfort horizontal plane = 0.93 (bony rhinion to subspinale) – 6
Deviated	Deviation of nose is opposite to the deviation of the nasal septum and in the same direction as the nasal spine (right or left)
Wide	Wider than the nose ridge. It is correlated with a short, wide, groovy, nasal spine and low, wide nasal foramen
Moderate	Equal to the width of the nose ridge
Narrow	It is correlated with a long, narrow, pronounced nasal spine and long, narrow nasal foramen
Rounded	Length of anterior nasal spine equal to or smaller than width of its base; tip of spine forming an obtuse angle
Pointed	Length of anterior nasal spine larger than width of its base; tip of spine pointed
Wing of the nose	
	The wing of the nose begins at the lateral edge of the piriform foramen at the level of nasal spine The height of the upper border of the alae is in line with the crista conchalis An exposed nasal septum is characteristic of a crest-shaped base of the nose
Medium	(Conchale to subspinale)/(supraorbitale to subspinale) = 0.21 ± 0.02

(continued)

Table 3.13 (continued)

Nose	
High	(Conchale to subspinale)/(supraorbitale to subspinale) > 0.23
Low	(Conchale to subspinale)/(supraorbitale to subspinale) < 0.19
Level	Left and right conchale and left and right lower points of the piriform aperture situated on the same level
Right higher	Right conchale or right lower point of the piriform aperture higher than left
Left higher	Left conchale or left lower point of the piriform aperture higher than right
Nasal bridge depth	
Medium	Sellion not much deeper than glabella to rhinion line
Large	Sellion much deeper than glabella to rhinion line
Small	Sellion on glabella to rhinion line
Nasal bridge breadth	
Medium	(Minimal breadth of nasal bones at nasal saddle level (57) + 6 mm)/(naso-gnathic left to naso-gnathic right + 6 mm) = 0.85 ± 0.04
Large	(Minimal breadth of nasal bones at nasal saddle level (57) + 6 mm)/(naso-gnathic left to naso-gnathic right + 6 mm) > 0.89
Small	(Minimal breadth of nasal bones at nasal saddle level (57) + 6 mm)/(naso-gnathic left to naso-gnathic right + 6 mm) < 0.81
Nasal saddle width	
Medium	(Naso-gnathic left to naso-gnathic right + 6 mm)/(canine left to canine right) = 0.38 ± 0.03
Large	(Naso-gnathic left to naso-gnathic right + 6 mm)/(canine left to canine right) > 0.41
Small	(Naso-gnathic left to naso-gnathic right + 6 mm)/(canine left to canine right) < 0.35
	Nasal ridge index = minimal breadth of nasal bone × 100/anterior length of nasal bone 10–30 = narrow; 30–45 = medium; 45–75 = broad

3.3.7 The Ear

Although there have been some studies relating ear morphology to skeletal structure, this facial feature is understudied. Gerasimov (1955) considered the angle of ear to be parallel to the jaw line and stated that when the mastoid processes are directed downward (in the Frankfort Horizontal Plane), the earlobe will be attached (adherent to the soft tissue of the cheek), whereas, where the mastoid processes point forward, the ear lobe will be free. However, recent dissection studies disagree as to the reliability of these standards; Renwick (2012) confirmed that adherent ear lobes relate to downward pointing mastoid processes, while studies using CT data showed no relationship between these features (Guyomarc'h and Stephan 2012). The confirmed standards are presented in Table 3.16.

Table 3.14 Anatomical standards relating to mouth shape

Mouth	
Width of the mouth	
	Equal to the distance between the mandibular second molars Mouth corners positioned on radiating lines (perpendicular to the palate arc) from the first premolar–canine junction Intercanine distance = 75% of overall mouth width The distance between the first premolars equal to mouth width Mouth corners positioned vertically below the infraorbital foramina
Medium	Estimated on regression equation mouth width/(bigonial breadth + 20 mm) = 0.52 ± 0.02
Large	Estimated on regression equation mouth width/(bigonial breadth + 20 mm) > 0.54
Small	Estimated on regression equation mouth width/(bigonial breadth + 20 mm) < 0.50
Position of the fissure	
	The closed fissure is positioned at the level of the upper edge of the anterior teeth of the mandible The open fissure is positioned at the mid-line of the maxillary incisors
Height of the lips	
	Approximately equal to the height of the enamel of the upper and lower incisors European: maximum upper lip height (mm) = 0.4 + (0.6 × max. maxillary tooth enamel height) European: maximum lower lip height (mm) = 5.5 + (0.4 × max. mandibular tooth enamel height) Indian subcontinent: maximum upper lip height (mm) = 3.4 + (0.4 × max. maxillary tooth enamel height) Indian subcontinent: maximum lower lip height (mm) = 6 + (0.5 × max. mandibular tooth enamel height)
Medium	(Subspinale to supradentale)/(supraorbitale to gnathion (2) + 6 mm) = 0.12 ± 0.011
High	(Subspinale to supradentale)/(supraorbitale to gnathion (2) + 6 mm) > 0.131
Low	(Subspinale to supradentale)/(supraorbitale to gnathion (2) + 6 mm) < 0.109
Width of the philtrum	
	The width of the philtrum corresponds to the distance between the midpoints of the upper central incisors
Prognathism	
Overbite or maxillary prognathism	The upper lip projects more anteriorly than the lower lip
An underbite or edge-to-edge occlusion	The lower lip protrudes more anteriorly than the upper lip

(continued)

Table 3.14 (continued)

Mouth	
Line between closed lips	
Arched (upward or downward)	The direction of these lines generally coincides with the line formed when the teeth are closed
Straight (upward or downward)	
Occlusion and malocclusion	
Edge-to-edge bite	Upper and lower anterior teeth fitting together edge-to-edge
Moderate overbite	Anterior upper teeth slightly projecting over lower ones
Roof-shaped	Marked overbite
Cornice-shaped bite	Marked maxillary and mandibular alveolar prognathism
Stepwise	Anterior mandibular teeth projecting anteriorly relative to anterior maxillary teeth
Gaping	Anterior maxillary and mandibular teeth curved and not fitting together
Oblique	Some teeth fit together normally, others show malocclusion

Table 3.15 Relationship between the zygomatic bones, the canine fossa, and the soft cheeks

Horizontal profile of the face	
	The cheekbones define the width of the face and its horizontal profile
	The horizontal profile of the face depends on the width and height of the curvature of the cheekbones, the depth of the canine fossae, and the nasomalar and zygomaxillary angles
Size of malar bones	
Medium	Malar bones medium width and gently inclined backward; (bizygomatic breadth (45) + 10 mm)/(minimal frontal breadth (9) + 10 mm) $= 1.37 \pm 0.03$
Large	Malar bones wide and frontally positioned; (bizygomatic breadth (45) + 10 mm)/(minimal frontal breadth (9) + 10 mm) > 1.40
Small	Malar bones narrow and inclined backward; (bizygomatic breadth (45) + 10 mm)/(minimal frontal breadth (9) + 10 mm) < 1.34
Smile line	
	The nose-cheek (nasolabial) fold extends from the upper edge of the nostril toward the upper first molar
Protrusion of the smile line	
	It depends on the depth of the following parts: • The canine fossa • The degree of horizontal face profiling • The projection of the frontal surface of the cheekbones • The presence or absence of teeth
Nose-cheek folds pronounced	The canine fossae are deep, and profiling of the face is strong
Depth of the canine fossa	
Shallow	Up to 3 mm
Moderate	Between 4 and 6 mm
Deep	Over 6 mm

Table 3.16 Relationship between ear morphology and skeletal structure

Ear	
	The tragus of the ear corresponds to the upper rim of the external auditory meatus
	The height of the ear approximates the length of the nose
Protrusion of the ear	
Upper	The supramastoid crest on the temporal bone is strongly developed and protrudes
Lower	The outer surface of the mastoid process is rough
Total	All these features are present
Lobe of the ear	
Lobe attached	The mastoid processes are directed downward when the skull is in the Frankfort horizontal plane
Lobe free	The mastoid points forward when the skull is in the Frankfort horizontal plane

3.3.8 The Chin

There are some standards relating the mental region of the mandible to chin shape (Balueva et al. 2009). These are presented in Table 3.17.

The facial proportions are an important element to understanding facial geometry. The aim of the facial proportion assessment is to establish the variation from the ideal dimensions of the human form. This, combined with anthropometric norms, gives information about facial features as a symmetrical and balanced pattern, based on statistical means taking into account variations in age, sex, and ancestry. In this way, George (1993) described facial proportions based on the studies of Farkas and Munro (1987), Powell and Humphreys (1984).

3.4 Examination Criteria for Craniofacial Superimposition

Assessment of the quality of the matching and anatomical consistency between the face and skeletal structures for CFS has been carried out following a number of different criteria. These include the works of Helmer (1987), Helmer et al. (1989), Powell and Humphreys (1984), Chai et al. (1989), Austin-Smith and Maples (1994), Yoshino et al. (1995), Yoshino (2012), Lan (1995), Jayaprakash et al. (2001), Ricci et al. (2006), Ishii et al. (2011), and Gordon and Steyn (2012). These criteria are presented in detail below.

3.4.1 Helmer (1984, 2012)

This method of assessment includes the use of several soft tissue thickness markers, attached to the skull along a vertical central line. Helmer employed average German

Table 3.17 Relationship between the mental region of the mandible and chin shape

	The presence of convexities in the lower part of the mandibular body is a notable feature both of the skull and of the face.
Width of the chin	
	This is defined by the degree of elevation in the mental region of the mandible and the width its base.
Shape of the chin	
High	The height of the mandibular body diminishes from the chin triangle to the rami.
Wide	Everted gonial regions of the mandible are associated with the wider variants of the lower face and more developed masseter muscles.
Height of the chin	
Medium	(Supramentale to gnathion + 6 mm)/(supraorbitale to gnathion + 6 mm)= 0.215 ± 0.015
Large	(Supramentale to gnathion + 6 mm)/(supraorbitale to gnathion + 6 mm) > 0.23
Small	(Supramentale to gnathion + 6 mm)/(supraorbitale to gnathion + 6 mm) < 0.20
	Chin height index = Height of the chin triangle $\times$ 100/Height of the ramus along the second premolar 100–110 = normal; 110–115 = high; 115–120 = very high
Chin prominence	
Straight	Most projecting point of chin slightly anterior to vertical line
Prominent	Most projecting point of chin markedly anterior to vertical line
Receding	Most projecting point of chin on vertical line or behind it
Width of the chin	
Medium	(Mentale left to mentale right)/(bigonial width + 20 mm)= 0.35 ± 0.02
Large	(Mentale left to mentale right)/(bigonial width + 20 mm) > 0.37
Small	(Mentale left to mentale right)/(bigonial width + 20 mm) < 0.33
Shape of the chin in frontal view	
Rounded	Outline rounded, genial tubercles unexpressed
Triangular	Outline pointed, genial tubercles close together
Square	Outline square, genial tubercles wide apart

soft tissue data (Helmer 1984) collected by ultrasound. These cephalometric landmarks (nasion, rhinion, gonion, gnathion) are then matched to the profile on the ante-mortem photograph. The alignment of these landmarks indicates a positive identification. Variations on this methodology have been employed. Bajnóczky and Királyfalvi (1995) suggested a digital method to mark the superimposed ante-mortem photograph and skull image. The coordinate values of these points were then recorded and expressed as pixel units. Birngruber et al. (2010) glued 53 markers to the skull to mark the tissue depth at each anthropological landmark (Helmer 1984). The skull and the ante-mortem photograph were then superimposed in order to assess whether or not the tissue markers matched with the contours of the face.

Table 3.18 Landmarks, lines, and profile curves suggested by Chai et al. (1984)

Landmarks on face and skull	Facial lines	Skeletal lines	Profile outlines
g: glabella	ex-ex	ec-ec	Cranial vault
tr: trichion	g-gn	g-gn	Brow ridge
v: vertex	se-se	se-se	Nasal
n: nasion	ch-ch	-gn-	Gonial angle
sn: subnasal	en-eh		Lower jaw
gn: gnathion	en-eh		Occipital
pg: pogonion	-gn-		Forehead
rhi: rhinion			Chin
ns: nasospinale			Zygomatic
pr: prosthion			
inf: infradentale anterior			
t: tragion			
eu: euryon			
al: alare			
che: cheilion			
en: endocanthion			
ex: exocanthion			
zy: zygion			
go: gonion			
ca: caninion			
se: superciliary			
ec: ectoconchion			

3.4.2 Chai et al. (2010)

This method is based on a study of 224 Chinese subjects (100 males and 124 females) aged between 18 and 55 years, from X-ray images. The protocol relies on the analysis of positional relationships between homologous facial and skull landmarks, the thickness of soft tissue at specific points, and the fit of facial outlines with the cranial structures. Fifty-two indices were established as a standard for CFS and identification (Table 3.18).

3.4.3 Austin-Smith and Maples (1994)

Two sets of 12 criteria are employed in this method to analyze skull-face consistency using lateral and frontal view photographs. Relevant soft tissue thickness data is also utilized along with the anatomical criteria. The authors suggest that with anterior dentition, skull/photograph superimposition is reliable when two or more photographs are used in the identification. The following features were used for a consistent fit between skull and face:

Lateral View

1. The vault of the skull and the head height must be similar.
2. The glabellar outline of both the bone and the soft tissue must have a similar slope, although the line of the face does not always follow the line of the skull exactly. There may be slight differences in soft tissue thicknesses that do not relate to nuances in the contour of the bone.
3. The lateral angle of the eye lies within the bony lateral wall of the orbit.
4. The glabella, nasal bridge, and nasal bone area is perhaps the most distinctive. The prominence of the glabella and the depth of the nasal bridge are closely approximated by the soft tissue covering this area. The nasal bones fall within the structure of the nose and the imaginary continued line, composed of the lateral nasal cartilages in life, will conform to the shape of the nose except in cases of noticeable deformity.
5. The outline of the frontal process of the zygomatic bones can normally be seen in the flesh of the face. The skeletal process can be aligned with the process seen in the face.
6. The outline of the zygomatic arch can be seen and aligned in those individuals with minimal soft tissue thickness.
7. The anterior nasal spine lies posterior to the base of the nose near the most posterior portion of the lateral septal cartilage.
8. The porion aligns posterior to the tragus and inferior to the crus of the helix.
9. The prosthion lies posterior to the anterior edge of the upper lip.
10. The pogonion lies posterior to the indentation observable in the chin where the orbicularis oris muscle crosses the mentalis muscle.
11. The mental protuberance of the mandible lies posterior to the point of the chin. The shape of the bone (pointed or rounded) corresponds to the shape of the chin.
12. The occipital curve lies within the outline of the back of the head. This area is usually covered with hair and the exact location may be difficult to judge.

Frontal View

1. The length of the skull from bregma to menton fits within the face. Bregma is usually covered with hair.
2. The width of the cranium fills the forehead area of the face.
3. The temporal line can sometimes be distinguished on the photograph. If so, the line of the skull corresponds to the line seen on the face.
4. The eyebrow generally follows the upper edge of the orbit over the medial two-thirds. At the lateral superior one-third of the orbit, the eyebrow continues horizontally as the orbital rim begins to curve inferiorly.
5. The orbits completely encase the eyes including the medial and lateral folds. The point of attachment of the medial and lateral palpebral ligaments can usually be found on the skull. These areas align with the folds of the eye.
6. The lacrimal groove can sometimes be distinguished on the photograph. If so, the groove observable on the bone aligns with the groove seen on the face.

7. The breadth of the nasal bridge on the cranium and surrounding soft tissue is similar. In the skull, the bridge extends from one orbital opening to the other. In the face, the bridge spreads between the medial palpebral ligament attachments.
8. The external auditory meatus opening lies medial to the tragus of the ear. The best way to judge this area is to place a projecting marker in the ear canal. On superimposition, the marker will appear to exit the ear behind the tragus.
9. The width and length of the nasal aperture falls inside the borders of the nose.
10. The anterior nasal spine lies superior to the inferior border of the medial crus of the nose. With advanced age, the crus of the nose begins to sag and the anterior nasal spine is located more superiorly.
11. The oblique line of the mandible (between the buccinator and the masseter muscles) is sometimes visible in the face. The line of the mandible corresponds to the line of the face.
12. The curve of the mandible is similar to that of the facial jaw. At no point does the bone appear to project from the flesh. Rounded, pointed, or notched chins will be evident in the mandible.

3.4.4 Yoshino et al. (1995, 2012)

This method evaluates the anatomical consistency between skull and face by means of video superimposition. The anatomical relationships and soft tissue thickness data is based on Ogawa's data (Ogawa 1960). The exact thicknesses of soft tissue at the anthropometrical points of the skull are measured on the superimposed transparent films by using a sliding caliper. Eighteen assessment criteria are used for the evaluation of the anatomical consistency between the face and the skull. The criteria used are divided into three types: outlines, soft-tissue thickness, and positional relationships (Tables 3.19, 3.20, and 3.21). The authors suggest a positive identification can be achieved if 13 or more criteria demonstrate concordance between the skull and the face.

3.4.5 Lan (1995)

This method is based on a study of 3123 subjects from 15 nationalities (1554 males and 1569 females), with one front view and one profile photograph of each subject. The method includes anthropometry from photographs and X-rays. A total of 69 indices are established for identification (Table 3.22). The authors noted that some indices showed significant differences between different nationalities: the distance between the vertical line of ectocanthion and gonion; the distance between gonions; and the thickness of the soft tissue at the trichion, opisthocranion, and sellion.

Table 3.19 Examination criteria for the assessment of anatomical consistency between the skull and the face

Outline	Soft tissue thickness	Positional relationships
1. Forehead line	1. Zygion	1. Distance from the supraorbital margin to the midline of eyebrow
2. Buccal line	2. Gnathion	2. Distance from the medial orbital margin to the endocanthion
3. Mandibular line	3. Pogonion	3. Distance from the lateral orbital margin to the ectocanthion
4. Nasal dorsum line	4. Gonion	4. Eye-slit standard ratio (eye-slit height from the lower orbital margin/orbital height)
–	5. Nasion	5. Distance from the lateral margin of nasal aperture to the ala
–	6. Rhinion	6. Distance from the lower margin of nasal aperture to the lowest portion of external nasal tip
–	7. Subnasale	7. Placement of the cheilion to upper teeth

Taken from Yoshino et al. (1995)

Table 3.20 Criteria for assessing anatomical consistency between skull and face in frontal view

Outline		Soft-tissue thickness		Positional relationship	
Skull	Face	Skull	Face	Skull	Face
Temporal line	Forehead	Zygion	Zygion	Supraorbital margin	Eyebrow
Lateral line of zygomatic bone	Cheek outline	Gonion	Gonion	Medial orbital margin	Endocanthion
Mandibular line	Lower jaw outline	Gnathion	Gnathion	Lateral orbital margin (Whitnall's malar tubercle)	Ectocanthion
–	–	–	–	Orbit	Eye-slit
–	–	–	–	Lateral margin of piriform aperture	Alare
–	–	–	–	Cutting edge of upper central incisor	Stomion
–	–	–	–	Teeth (premolar)	Cheilion
–	–	–	–	Occlusal line	Oral slit

Taken from Yoshino (2012)

3.4.6 Jayaprakash et al. (2001)

This is a craniofacial morpho-analytical approach, based on the shape correlation between the skull and face photograph. This approach relies on previous work developed by Lan (1995), İşcan (1993), Farkas (1981), and George (1987, 1993) and special attention is placed on the nasal region. The facial and skull traits and attributes, and the measurements employed for this study are detailed in Tables 3.23, 3.24, and 3.25.

Table 3.21 Criteria for assessing anatomical consistency between skull and face in lateral/oblique view

Outline		Soft-tissue thickness		Positional relationship	
Skull	Face	Skull	Face	Skull	Face
Frontal bone contour	Forehead outline	Trichion	Trichion	Supraorbital margin	Eyebrow
Outline from nasion to rhinion	Nasal dorsum line	Glabella	Glabella	Lateral orbital margin (Whitnall's malar tubercle)	Ectocanthion
Mental outline	Chin outline	Nasion	Nasion	Nasion	Higher than nasal root
Gonial outline	Jaw angle outline	Rhinion	Rhinion	Lateral margin of piriform aperture	Alare
–	–	Slightly inferior to nasospinale	Subnasale	Lower margin of piriform aperture	Subnasale
–	–	Pogonion	Pogonion	Incisor	Stomion
–	–	Gnathion	Gnathion	Teeth (canine premolar)	Cheilion

Taken from (Yoshino et al. 1995)

3.4.7 Ricci et al. (2006)

The authors presented an algorithm for identification using CFS. Fourteen subjects and their matching facial photographs and skull radiographs were selected. The algorithm calculated the distance of each transferred cross (anatomical points) and the corresponding average. Their results indicate that the smaller the mean value, the greater the index of similarity between the face and the skull. A total of 196 cross-comparisons were carried out. The following tables present the anatomical points that were located and marked with a cross on each facial image (Tables 3.26 and 3.27).

3.4.8 Ishii et al. (2011)

This method was based on a study of three subjects, a young man (23 years old), a man with an edentulous upper jaw (36 years old), and a woman (40 years old), using 3D CT data for CFS. Miyasaka (1987), Suzuki (1948), and Ichikawa (1975) studies were used for the morphological assessment technique (Table 3.28).

Table 3.22 Lines, landmarks and index from Lan (1995)

Determining lines	Landmarks index	Index of soft tissue thickness	Index number of index
1. Ectocanthion line. Between two ectocanthions, used as a horizontal base line to mark the horizontal relationship of the superimposition.	Superciliary and supraorbital line	Vertex	Endocanthion: Distance between endocanthion and supraorbital/orbital height
2. Front central line. From glabella to gnathion, vertical to the ectocanthion line, used to mark the vertical relationship of the superimposition.	Orbital height	Euryon	Ectocanthion: Distance between ectocanthion and supraorbital/Orbital height
3. Superciliary line. Between two superciliaries, parallel with the ectocanthion line, and vertical to the front central line.	Ectocanthion and supraorbital line	Zygion	Distance between Endocanthions: Distance between bi-endocanthions/ Distance between junctures of external orbit
4. Subnasal line. At the subnasale, vertical to the front central line, used to mark the superimposition of subnasale and infra-apertura piriformis.	Endocanthion and supraorbital line	Tragion	Distance between Ectocanthions: Distance between bi-ectocanthions/ Distance between junctures of external orbit
5. Cheilion line. Between two cheilions, vertical to front central line, used to mark the superimposition of cheilion and maxillary teeth.	Subnasale and infra-apertura piriformis	Gonion	Stomion line: Distance between supradental alveolus and stomion line/Distance between infradental alveoli and stomion line
6. Gnathion line. At gnathion, vertical to the front central line, used to mark the superimposition of soft tissue of gnathion and pogonion.	Cheilion line and infra-apertura piriformis	Gnathion	Distance between gonions: Distance between gonions on skull/Distance between gonions on human image
7, 8. Endocanthion vertical lines (left and right). From the endocanthion line to the cheilion line, parallelwith the front central line, used to mark the relationship of endocanthion and maxillary teeth.	Endocanthion vertical line to maxillary tooth (left)	Opisthocranion	Distance between cheilions: Distance between cheilions/ Distancebetween gonions on skull
9, 10. Ectocanthion vertical lines (left-right). From the ectocanthion line to the gonion line, parallel with the front central line, and are	Endocanthion vertical line to maxillary tooth (right)	Trichion	–

(continued)

Table 3.22 (continued)

Determining lines	Landmarks index	Index of soft tissue thickness	Index number of index
used to mark the horizontal superimposition of ectocanthion and gonion.			
Morphological curves include the following: (1) head vault curve, (2) arcus superciliary curve, (3) nose curve, (4) lower jaw curve,(5) gonion curve, (6) head back curve, (7) forehead curve, (8) pogonion curve, and (9) zygomatic curve.	Distance between two junctures of external orbit	Glabella	–
–	Distance between bi-endocanthions	Nasion	–
–	Cheilion to mandibular tooth	Sellion	–
–	Ectocanthion and endoconchion	Subnasale	–
–	Prosthion and cheilion line	Pogonion	–
–	lnfradentale anterius and cheilion	–	–
–	Distance between gonions	–	–
–	Distance between gonions on the skull	–	–
–	Distance between zygions	–	–
–	Distance between cheilions	–	–
–	Gonion and tragion on the skull	–	–
–	Gonion and ectocanthion vertical line on the skull	–	–

Table 3.23 Facial and skull measurements and indices (a)

Measurement details and indices of facial skull		Cranioscopic observations in the skull [visual (v) and mensural (m)] in comparison with the chepaloscopic observations from the facial photograph (visual)							
		Skull	Photo	Skull	Photo	Skull	Photo	Skull	Photo
		Face	Face (v)	Orbit	Eyes (v)	Nasal area	Nose (v)	Malar bone	Cheek (v)
Vertical	n-gn n-pr n-rhi rhi-ns n-ns orb-ht	**Facial Ht (m).** Short. S Medium. M Long. L **Contour (v).** Elliptical. E Ovoid. O Round. R Quadra. Q Pentago. P Asy. A.R.L	**Facial Ht** Short Medium Long **Contour** Elliptical Ovoid Round Square Pentago Asy. A.R.L	**Orb. Profile (v)** Weak. W Mod. Weak.E Mod. Strong. S **Brow. Ridge. med (v)** Straight. A Arched. B Angular. C Asy. A.R.L	**Eyes** Prom. Mod.Prom Mod.Deep Deep **Eye Brow med** Straight Arched Angular Asy. A.R.L	**Na.Area (m)** Narrow. N Medium. M Broad. B Asy. A.R.L **Na. Notch (v)** Deep.D Mod.M Slight.S Smooth.A	**Nose** Narrow Medium Broad Asy.A.R.L **Root** Prom. Mod. Slight Absent	**Malar(v)** Prom.P Medium.M Shallow.S Asy.A.R.L **Zygomatic Arch(v)** V.prot.V Prot.P Mod.M Reced.R Asy.A.R.L	**Cheek** Prom. Medium Shallow Asy.A.R.L **Zygoma** V.Prom Prom. Mod. Smooth Asy.A.R.L
Horizontal	ft-ft ect-ect mf-ect mf-mf zy-zy go-go ecm-ecm bdth. na. ridge na. bdth	**Fr. lines (v)** Prom. P Mod. M Shallow. S **Fr. Emin (v)** Prom. P Mod. M Incip. I Absent. A	**Fr. lines** Prom. Mod. Incip. **Fr. Prot** Prom. Mod. Incip. Absent **L. Face**	**Brow Ridge. lat (v)** Straight. A Arched. B Angular. C Asy. A.R.L **Ecto/Endo. Axis (v)** Horizontal. H Oblique	**Eye brow last** Straight Arched Angular Asy. A.R.L **Eye opening Axis** Horizontal Oblique	**Na.Ridge** Straight.S Prom.P Convex.X Concave.C Wavy.W Asy. A.R.L **Ri.Bdth** Narrow.N Medium.M	**Bridge** Straight.S Prom.P Convex/ Hump Concave Wavy Asy. A.R.L **Br.bdth** Narrow	**Can.Fos. (v)** Prom.P Mod.M Shallow.S	**Smile/Nor No. Ch.Fold** Con. Mod. Incip.

(continued)

Table 3.23 (continued)

Measurement details and indices of facial skull		Cranioscopic observations in the skull [visual (v) and mensural (m)] in comparison with the chepaloscopic observations from the facial photograph (visual)							
		Skull	Photo	Skull	Photo	Skull	Photo	Skull	Photo
		Face	Face (v)	Orbit	Eyes (v)	Nasal area	Nose (v)	Malar bone	Cheek (v)
		Mandible G.A.C.C.R. (m) Lower. L Equal. E Higher. H	Round Oval Triangular	Internal. I External. E Asy. A.R.L	Internal External Asy. A.R.L	Broad.B **Ri.Prom** Low.L Medium.M Raised.R	Medium Broad **Br.Prom** Low Medium Raised		
Others	ba-pr ba-na lgth. jaw bi-cdl pr-alv ol-sta	**Mand Form (v)** Narrow. N Medium. M Broad. B Asy. A.R.L **Roc. Jaw (v)** P.A	**JawContour** Narrow Medium Broad Asy. A.R.L **L.J.P.P.A**	**Overhang (V)** Complete. C Medial. M Lateral. L Central. E Absent. A	**Eye Folds** Complete Medial Lateral Central Absent	**Lat.Dep.P.A** **Lat.Bul.P.A** **Pl.Ap. (m)** Narrow.N Medium.M Broad.B Asy.A.R.L **Gut.Evi.P.A** ns.level. Low Medium High	**Lat.Dep** **Lat.Bulge Alae** Narrow Medium Broad Asy.A.R.L Exposed Nostril A/P	–	–

Indices	T. Facial U. Facial Mand. Orbital Inter. Orb Nasal Na. ridge Max. Alv Palatal Alveolar Chin ht.	**Gon. Evr. (v)** V. Prom. V Prom. P Mod. M Incip. I Asy. A.R.L **Chin. W. (v)** Narrow. N Mod. M Broad. B **Chin. H. (m)** Rami. Ht. (m) Diff. High. H Normal. N High Mand	**P.L.P** V. Prom Prom Mod. None Asy. A.R.L **Chin. W.** Narrow Mod. Wide Chin. Ht. High Normal High Chin			**Pi.Edge(v)** Low.L Mod.M Raised.R **Na.Base** Straight.S Al.Arched. L Arched.A **Spine (v)** N/M/B **Sp.dir** Horizontal. H Upwar.U Downward. D Asy.A.R.L	**Alar edge** Flat Mod. Raised **Septum** Exposed Par. Exposed Unexposed **Na.tip** S/M.S/B **Na.tip.dir.** Horizontal Upward Downward Asy.A.R.L	–	–

Taken from Jayaprakash et al. (2001)

Table 3.24 Facial and skull measurements and indices (b)

Measurement details and indices of facial skull		Cranioscopic observations in the skull [visual (v) and mensural (m)] in comparison with the chepaloscopic observations from the facial photograph (visual)					
		Skull	Photo	Skull	Photo	Skull	Photo
		Alv. Edge	Lips (v)	Max. Alv. zone	Mouth (v)	Mastoid areas	Ear (v)
Vertical	n-gn n-pr n-rhi rhi-ns n-ns orb-ht	**Alv.Edge(v)** Prot.Upper.U Prot.Lower.L Prot.Total.T Normal.N Sheer(u/l).S **Teeth(v)** UpperProt.U Lower Prot.L Both Prot.B Both Nor.N Edge-Edge.E	**Lips** Prot Upper Prot Lower Prot.Total Normal Flat(u/l) **Teeth** Upper Prot. Lower Prot. Both Prot. Both Nor. Normal	**Index(m)** Narrow.N Medium. M Broad. B **Overbite(v)** Maxillary.X Mandibular.M Edge-Edge.E Normal.N Asy.A.R.L	**Mouth** Narrow Medium Broad **Protrusion** Upper Lower Total Normal Asy.A.R.L	**Mas.tip(v)** Con.Down.C Downward.D Forward.F **Mas.&S.M.Cr.Prot(v) S. M.** V.Prom.V Prom.P Normal.N Incip.I	**Ear Lobe** Attached Par. Attached Free **Helix.Prot Upper** V.Prot Prot Mod Least
Horizontal	ft-ft ect-ect mf-ect mf-mf zy-zy go-go ecm-ecm bdth. na. ridge na. bdth	**Present/Edentulous** Trema Diastema Afrition Conoid Overriding/ Protruding Tooth	**Exposed/ Unexposed** Trema Diastema Afrition Conoid Overriding/ Protruding Lip.Clo.Line Asy.A.R.L	**Overrid.Teeth/Prot (v)** Absten.A Maxilla.X Mandible.M Right.R Left.L	**Lip.Clo. Line** Absent Upper Lower Right Left	**Mastoid(v)** V.Prom.V Prom.P Normal.N Incip.I	**Lower** V.Prot Prot. Mod. Least

Indices	T. Facial U. Facial Mand. Orbital Inter. Orb Nasal Na. ridge Max. Alv Palatal Alveolar Chin ht.	

Taken from Jayaprakash et al. (2001)

Alv alveolar, *Asy* asymmetry, *A.R.L* absent.right.left, *B* broad, *Br* bridge, *Bul* bulge, *Can.For* canine fossa, *Clo* closure, *Con* conspicuous, *Cr* crest, *C.C.R* coronoid-Condyle relationship, *D* vertical distance det. Ectocanthus-Tragion, *Dep* depression, *Diff* difference, *Emin* eminence, *Evr* eversion, *Fr* frontal, *G.A* gonial angle, *Gon* gonial, *Gut. Evt* gutter evidence, *H/HT* high/height, *Incip* incipient, *L/R* left & right ectocanthus to nasion distance ratio, *Lat* lateral, *L* lower, *L.J.P* lateral jaw prominence, *Mand* mandibular, *Mas* mastoid, *Med* medial, *Mod* moderate, *M.S* mod.ly sharp, *Na* nasal, *No Ch* nose cheek, *Nor* normal, *Nost* nostni, *Par* partly, *Pentago* pentagonoid, *Phil* philtrum, *Pl. Ap* piriform aperture, *Pl. Edge* piriform aperture, *Prom* prominent, *Prot* protrusion, *P.L.P* postero lateral prominence, *Quedra* quadrangular, *Reced* receding, *Ri* ridge, *Rid* riding, *Rob* robust, *Roc* rocker, *S* sharp, *SL* slight, *Sp. dir* spine direction, *S.M* supra mastoid, *U/L* upper/lower, *V. prom* very prominent, *W* width

Table 3.25 The criteria used for assessing the fit the skull with the face photograph during superimposition are the following

Outline and soft tissue thickness				Positional relationship			
Frontal view		Lateral view		Frontal view		Lateral view	
Skull	Photo	Skull	Photo	Skull	Photo	Skull	Photo
Temporal line	Forehead	Frontal bone contour	Forehead outline	Frontal breadth	Breadth of forehead	Temporal line prominence	Temporal line imprint in the forehead
Zygomatic arch	Zygion	Nasion	Root of nose	Medial part of supraorbital ridge	Upper edge of medial portion of eyebrows	Medial part of supraorbital margin	Upper edge of medial portion of eyebrows
Lateral edge of piriform aperture	Lateral edge of alare	Inferior border of piriform aperture	Alar baseline	Lateral part of supraorbital margin	Lower edge of lateral part of the eyebrows	Lateral part of supraorbital margin	Lower edge of lateral part of eyebrow
Nasal spine	Tip of nose	Nasal spine	Tip of nose	Nasion	Higher than the root of nose	Nasion	Higher than the root of nose
Occlusal line	Lip closure line	Occlusal line	Lip closure line	Whitnall's tubercle	Precisely aligns with the ectocanthus on the horizontal plane, vertically the ectocanthus lies medial to the tubercle	Whitnall's tubercle	Lies posterior to the ectocanthus on the same horizontal plane
Mandibular outline	Lower jaw	Gonial outline	Jaw angle outline	Breadth of piriform aperture	Inner to alar breadth	Edge of piriform aperture	Posterior to the edge of ala
Mental outline	Chin outline	Mental outline	Chin outline	Nasal spine	Superior to the medial part of tip of nose	Occlusal line	Lip closure line
General outline of the skull	Fills the face photograph	General outline of the skull	Fills the face photograph	Zygion	Zygion	Nasal spine	Superior to the medial part of tip of nose
Auditory meatus	Medial to the upper edge of tragus on the same horizontal plane	Auditory meatus	Lateral to the upper edge of tragus on the same horizontal plane	Occlusal line	Lip closure line	Gonial flare	Jaw angle outline
				Gonial flare	Postero-lateral jaw prominence		

Taken from Jayaprakash et al. (2001)

Table 3.26 Anatomical points of the face

Anatomical points of the face
Eyebrow midpoint
Midpoint of the inferior margin of the palpebra inferior (lower eyelid)
Inner canthus
Outer canthus
The most forward point of the midsagittal plane (located between the two eyebrows)
Point below the inferior margin of the cartilaginous septum of the nose
Superior margin of the upper lip midpoint
Inferior margin of the lower lip midpoint
Zygoma

Table 3.27 Points of the skull X-rays

Points of the skull X-rays
Arcus superciliaris midpoint (superciliary arch)
Inferior orbital rim midpoint
Inner canthus, placed 3 mm medially to the medial wall of the orbit1 or against the medial wall of the orbit2 or 2–3 mm laterally to the lacrimal crest and 4–5 mm below the dacryon (junction of the lacromaxillary suture and the frontal bone)3
Outer canthus, placed 5 mm laterally to the orbit margin1 or 3–4 mm medially to the "Whitnall's malar tubercle"3; the "Whitnall's malar tubercle," placed on the orbital surface of the zygomatic bone 11 mm below the frontozygomatic suture, is the site of attachment of the rectus lateralis bulbi muscle, suspensory ligament, and levator palpebrae superioris muscle 4
Glabella
Inferior margin of the nasal spine
Upper infradental point (between the two medial upper incisors)
Lower infradental point (between the two medial lower incisors)
Zygomatic process of the maxilla

Table 3.28 Anthropometrical points used for each individual

Landmarks	
n	R-ex
R-zy	L-ex
L-zy	sn-ns
gn	R-al
R-go	L-al
L-go	R-ch
R-en	L-ch
L-en	–

n nasion, *R-zy* right zygion, *L-zy* left zygion, *gn* gnathion, *R-go* right gonion, *L-go* left gonion, *R-en* right endocanthion, *L-en* left endocanthion, *R-ex* right exocanthion, *L-ex* left exocanthion, *sn-sn* subnasal-subnasal, *R-al* right alare, *L-al* left alare, *R-ch* cheilion, *L-che* left cheilion

Table 3.29 Orientation, primary, and secondary landmarks

Methods	Description
Orientation landmarks	
Ectocanthion (ec)	Should overlap: used to define the orientation
Subnasal point (ns)	
Nasion (n)	
Primary landmarks	
Glabella (g)	Expected to be very close on skull and face, landmarks should touch or overlap
Dacryon (d)	
Frontotemporale (ft)	
Secondarylandmarks	
Gonial angle (go)	Bone and soft tissue landmarks not expected to overlap exactly but bony landmarks should be inside soft tissue landmarks
Gnathion (gn)	
Zygion (zy)	
Nasal aperture width/ alare (al)	

The description of the landmark on the skull (bony landmark) and the corresponding soft tissue landmark is given. Taken from Gordon and Steyn (2012)

3.4.9 *Gordon et al. (2006)*

The authors studied three methods: basic morphological matching (Austin-Smith and Maples 1994), landmark matching, and a combination of both approaches. The bony and soft tissue landmarks used were based on Martin and Saller (1957) and Farkas (1981). They proposed three different sets of landmarks for orientation and evaluation purposes for CFS (see Table 3.29).